ornl

ORNL/TM-10824

OAK RIDGE
NATIONAL
LABORATORY

MARTIN MARIETTA

Preliminary ANS Reactor Cold Source Gain Factor Calculations for Liquid Deuterium and Liquid Nitrogen-15

D. L. Henderson

OAK RIDGE NATIONAL LABORATORY
CENTRAL RESEARCH LIBRARY
CIRCULATION SECTION
4500N ROOM 175
LIBRARY LOAN COPY
DO NOT TRANSFER TO ANOTHER PERSON
If you wish someone else to see this report, send in name with report and the library will arrange a loan.

OPERATED BY
MARTIN MARIETTA ENERGY SYSTEMS, INC.
FOR THE UNITED STATES
DEPARTMENT OF ENERGY

Printed in the United States of America. Available from
National Technical Information Service
U.S. Department of Commerce
5285 Port Royal Road, Springfield, Virginia 22161
NTIS price codes—Printed Copy: A03; Microfiche A01

This report was prepared as an account of work sponsored by an agency of the United States Government. Neither the United States Government nor any agency thereof, nor any of their employees, makes any warranty, express or implied, or assumes any legal liability or responsibility for the accuracy, completeness, or usefulness of any information, apparatus, product, or process disclosed, or represents that its use would not infringe privately owned rights. Reference herein to any specific commercial product, process, or service by trade name, trademark, manufacturer, or otherwise, does not necessarily constitute or imply its endorsement, recommendation, or favoring by the United States Government or any agency thereof. The views and opinions of authors expressed herein do not necessarily state or reflect those of the United States Government or any agency thereof.

ORNL/TM-10824

Engineering Physics and Mathematics Division

PRELIMINARY ANS REACTOR COLD SOURCE GAIN FACTOR CALCULATIONS FOR LIQUID DEUTERIUM AND LIQUID NITROGEN-15

D. L. Henderson

Oak Ridge National Laboratory
P.O. Box 2008, MS 363
Oak Ridge, Tennessee 37831

DATE PUBLISHED — November 1988

Prepared by
Oak Ridge National Laboratory
Oak Ridge, Tennessee 37831
operated by
MARTIN MARIETTA ENERGY SYSTEMS, INC.
for the
U.S. DEPARTMENT OF ENERGY
under Contract No. DE-AC05-84OR21400

MARTIN MARIETTA ENERGY SYSTEMS LIBRARIES

3 4456 0283785 7

CONTENTS

ABSTRACT v

1. INTRODUCTION 1

2. CROSS-SECTION DATA AND LIBRARIES 3

3. COLD SOURCE GAIN FACTOR ANALYSIS 5

   3.1. SLAB MODERATORS 5

   3.2. SOLID SPHERE MODERATORS 8

   3.3. SPHERICAL SHELL MODERATORS 8

4. SUMMARY 13

5. ACKNOWLEDGMENT 15

REFERENCES 17

ABSTRACT

Individual energy group gain factors are computed for liquid nitrogen-15 and liquid deuterium cold source moderators using simple one-dimensional slab and spherical geometry calculational models. The energy spectrum of the neutron source is assumed to be that of a thermalized maxwellian flux at 20°C. The slab geometry calculations indicate that the optimum thickness for neutron transmission through a slab given an isotropic incident flux is for wavelengths above .6 nm, approximately .20 m for liquid deuterium and between .28 and .32 m for liquid nitrogen-15. The gain factors at .8 nm corresponding to these thicknesses are 15.5 for liquid deuterium and 3.50 for liquid nitrogen-15. The spherical geometry analysis showed that the cold neutron current below 10 meV of 1.36 n/m^2-s for the neutron component entering the cavity of a .16 m thick liquid deuterium spherical shell exceeds the neutron leakage current of 1.08 n/cm^2-s from a .38 m diameter liquid deuterium solid sphere. However, the cold neutron factors for the neutron entering the void region are considerably lower than for the solid sphere case.

1. INTRODUCTION

The Advanced Neutron Source (ANS) Reactor is a proposed research facility [1] designed to provide users with an intense steady state neutron source for neutron scattering experiments. One of the major areas of research to be carried out at the facility is that of cold neutron scattering. Cold neutrons are defined as neutrons that are in the wavelength band of .4 to 1.2 nm which corresponds approximately to the energy band .5 to 5 meV. For a research reactor operating at room temperature ~293 K and in which the neutrons have achieved a nearly maxwellian energy distribution, the fraction of neutrons available within the wavelength band of interest is approximately 1.7% of the total neutron population. This usually translates into a low intensity cold neutron beam available for experiments. To enhance the fraction of cold neutrons for experimental use within the wavelength band of interest, a special neutron moderating device called a cold source is used to bring neutrons into partial thermal equilibrium with the low temperature moderating material. A sketch of the reactor core and cold source positioned in a heavy water reflector tank extending approximately 1.5 m from the active core is shown in Figure 1. The heavy water reflector tank is surrounded by a light water pool.

The primary cold source moderating material considered for the ANS facility is liquid deuterium (LD_2), operating at a temperature of approximately 20 K. Safety concerns related to the use of liquid deuterium as the cold source moderator have led to the investigation of isotopic liquid nitrogen–15 (LN_2) as a possible alternative moderator. Liquid nitrogen–15 has several desirable characteristics for a cold source moderating material [2]:

a. it is a molecular liquid, so rotational levels are available for final thermalization at the low energy end of the spectrum;
b. the first solid phase is plastic, so that rotational levels would remain available if a colder solid moderator were possible;
c. it has good refrigeration characteristics;
d. it is non-inflammable; and
e. it has a very low thermal neutron capture cross section $\sigma_a = 2.4 \times 10^{-5}$ barns.

Since the atomic mass and the temperature of the moderating material both influence the cold neutron energy spectrum, two unfavorable characteristics are:

a. its atomic mass of 15 as compared to 2 for deuterium; and
b. the temperature of its liquid range being 63–77 K versus 14–20 K for deuterium.

To investigate the performance of a possible liquid nitrogen–15 versus a liquid deuterium cold source, individual energy group gain factors are computed for each moderatoring material in simple one-dimensional slab and spherical geometry parametric calculations. The slab geometry calculations allows one to examine the degree of neutron transmission (optimal thickness for transmission) and reflection by placing an isotropic flux of neutrons directed into the slab on one side and a vacuum boundary condition on the other. The ideal situation, that of a moderator immersed within an isotropic and spatially uniform density flux of neutrons is investigated by a spherical geometry model. Both solid and hollow spheres are considered. The energy spectrum of the neutron source is assumed to be a thermalized maxwellian flux at room temperature. These calculations represent an estimate of the enhancement that can be achieved both by direct transmission and by a moderator surrounded by an isotropic flux. In regard to the ANS reactor cold source, the results obtained are considered preliminary as the neutron source and cold source geometry used in the one-dimensional calculations do not correspond to the actual ANS reactor neutron source energy and spatial distributions and cold source geometry.

A brief discussion of the cross-section data and generated libraries used in the transport calculations is given in Section 2. Section 3 contains a description of the transport codes and calculational models used in the computations. A discussion of the gain factor results for the different geometries is also contained therein. This is followed by a brief summary in Section 4.

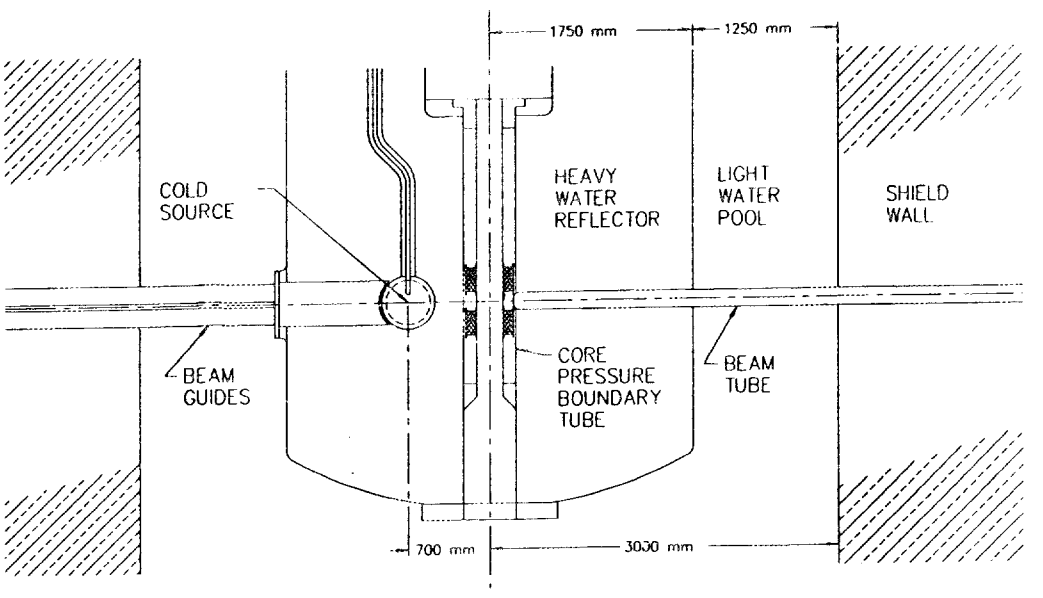

Figure 1. A sketch of the reactor core and cold source positioned in a heavy water reflector tank. The reflector tank is centered in a light water pool.

2. CROSS-SECTION DATA AND LIBRARIES

The cold neutron cross-section data for deuterium was generated using the YK (Young and Koppel) theoretical model [3] and incorporated into the ANSL-V cross-section data library [1,4]. A comparison of the ORNL point-wise data and the experimentally measured deuterium total scattering cross-section data (@ 19 K)[5] is shown in Figure 2. One notes that the ORNL data compares quite well with the experimental data in the energy range 7 to 100 meV. Between 3 to 7 meV, the agreement is fair and below 3 meV, the agreement is quite poor. This inadequacy of the YK model to represent the scattering cross-section data at low energies has been noted by several authors [6,7,8]. A new neutron scattering model is under investigation to improve upon the ORNL cross-section data below 7 meV.

A 15 group P_0 deuterium thermal energy cross-section data set was prepared from a 39 group ANSL-V data library for the gain factor thermalization calculations. The thermal energy groups are flux weighted by a maxwellian distribution at 20 K and contain neutron upscattering data. The energy boundaries of the 15 group cross-section set are given in Table 1. A liquid deuterium (LD_2) density of 0.1713 g/cm^3 and a 20% void fraction are used in the calculations.

A preliminary 15 group P_0 nitrogen–15 cross-section set was generated from a theoretical estimate of the double differential scattering cross section [2,9] by using the cold neutron scattering model for homonuclear diatomic liquids by V. F. Sears [10,11] and the liquid nitrogen total structure measurements by A. H. Narten et al. [12]. The nitrogen–15 group cross-section data set is flux weighted by a maxwellian distribution at 65 K and includes neutron upscattering data. The nitrogen–15 data set is quite preliminary as the cross-section data have not been experimentally verified. A liquid nitrogen–15 (LN_2) density of 0.922 g/cm^3 is used in the calculations.

An indication of the shape and magnitude of the nitrogen–15 total scattering cross section at 77 K as calculated by the above model is given in Figure 3. Here, the computed values are compared to the experimentally measured deuterium total scattering cross-section values (@ 19 K). One notes from the figure that the calculated nitrogen–15 values are quite similar in magnitude to the deuterium values. This qualitatively reflects the trend that one notes from the ENDF/B-V cross-section data library for which the absorption and total cross-section values at 25 meV are given in Table 2.

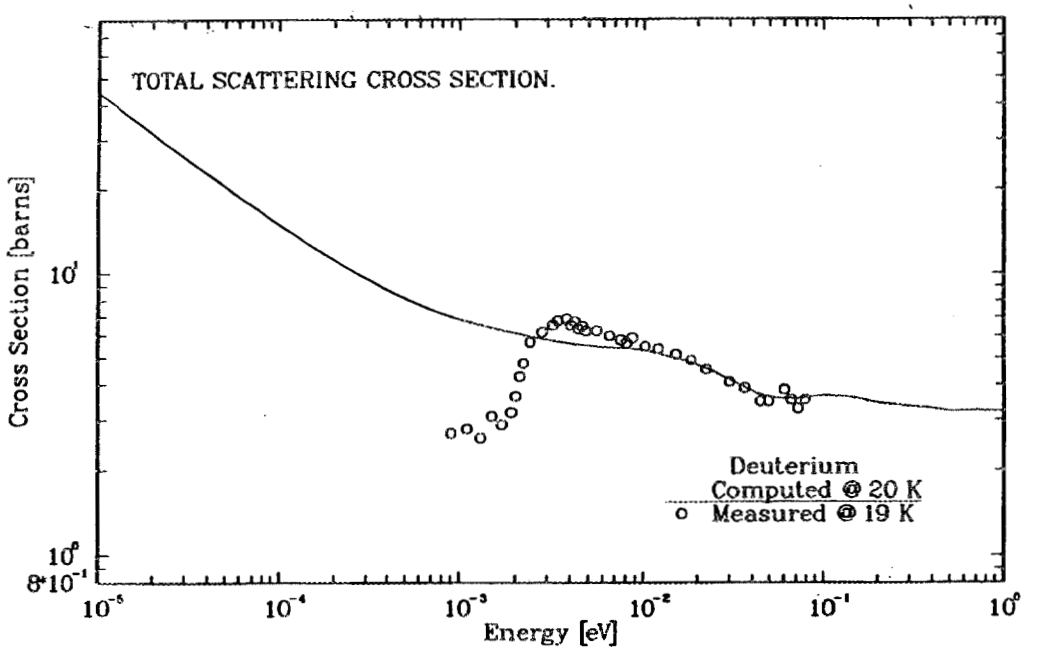

Figure 2. A comparison of the ORNL point-wise and the experimentally measured total scattering cross section data for deuterium.

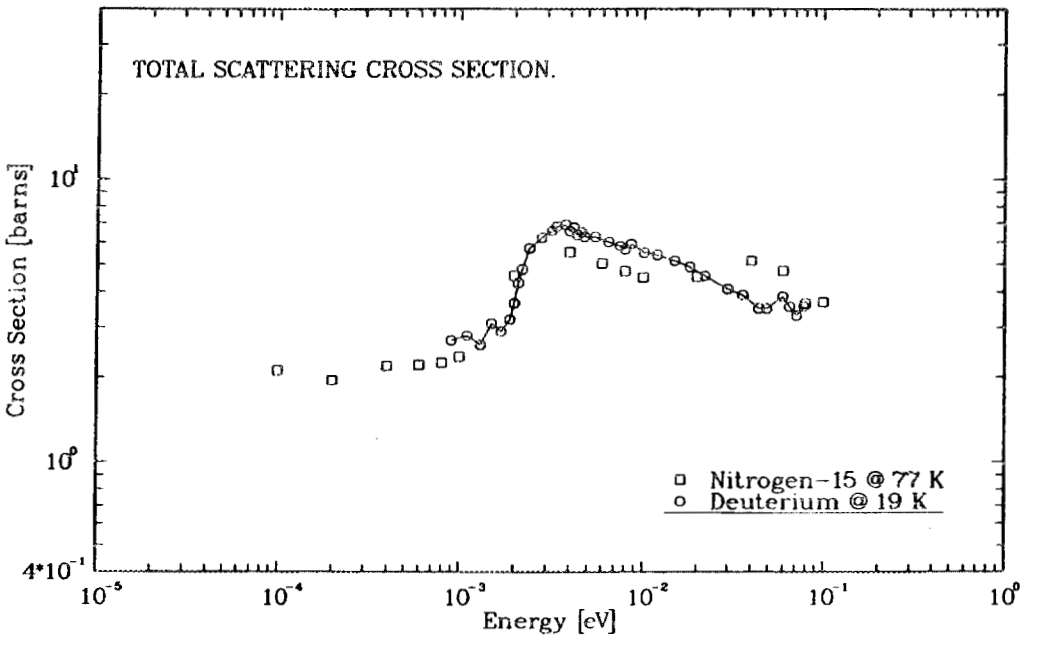

Figure 3. A plot of the experimental deuterium total cross section data and the calculated nitrogen–15 total cross section data.

Table 1

	Energy [meV]			Wavelength [nm]		
Group	High	Low	Midpoint	High	Low	Midpoint
1	215	162	188.5	0.071	0.062	0.066
2	162	104	133	0.089	0.071	0.080
3	104	50	77	0.128	0.089	0.108
4	50	30	40	0.165	0.128	0.147
5	30	10	20	0.286	0.165	0.226
6	10	4.45	7.23	0.429	0.286	0.358
7	4.45	3.25	3.85	0.502	0.429	0.465
8	3.25	2.60	2.93	0.561	0.502	0.531
9	2.60	2.15	2.38	0.617	0.561	0.589
10	2.15	1.80	1.98	0.674	0.617	0.646
11	1.80	1.45	1.63	0.751	0.674	0.713
12	1.45	1.15	1.30	0.844	0.751	0.797
13	1.15	0.85	1.00	0.981	0.844	0.912
14	0.85	0.55	0.70	1.220	0.981	1.101
15	0.55	0.01	0.28	9.046	1.220	5.133

Table 2

Deuterium and Nitrogen–15 Absorption and
Total Cross Section Values at 25 meV

	Nitrogen–15	Deuterium
Total (barns)	4.414	3.396
Capture (barns)	2.4×10^{-5}	5.06×10^{-4}

3. COLD SOURCE GAIN FACTOR ANALYSIS

In this section, cold neutron gain factor results are presented for homogeneous density liquid deuterium (LD_2) and liquid nitrogen–15 (LN_2) cold source moderators. The temperature of the moderators is assumed to be 20 K for deuterium and 65 K for nitrogen–15. Slab, solid sphere, and spherical shell moderators are considered. The energy spectrum of the neutron source is assumed to be a thermalized maxwellian at 20 C (293 K). The primary quantities of interest in the calculations are the energy group leakage spectra at the boundaries of the moderator from which the individual group gain factors are computed. The group gain factors are defined as

$$\text{Gain Factor (g)} = \frac{\text{neutron leakage in group g}}{\text{number of source neutrons in group g}} \ .$$

The calculations are normalized to one incoming neutron and are performed using the ANISN [13] and DOT [14] transport codes.

3.1. SLAB MODERATORS

A simple one-dimensional (variation of the flux in one spatial dimension) slab geometry calculational model is employed for the liquid deuterium and liquid nitrogen–15 cold source parametric transmission computations. Deuterium slabs having thicknesses of .05, .10, .15, .20, and .25 m and nitrogen–15 slabs of .16, .20, .24, .28, and .32 m are examined. The neutron source is assumed to be an isotropic flux of neutrons (for $\mu > 0$) incident on the slab from the left with a vacuum boundary condition on the right.

Figures 4 and 5 display the transmitted and reflected liquid deuterium cold neutron gain factor results plotted according to their group midpoint wavelengths. For the transmitted results at the longer wavelengths (> .60 nm), the maximum transmitted gain factor is achieved for a slab of thickness .20 m. Below .60 nm slabs with thicknesses of .15, .20, and .25 m give similar results. At .35 nm, the results are approximately equal for all thicknesses. For the reflected results, the gain factor values increase at all wavelengths as the slab thickness increases though the increase is less for the same step increase in size. This is reasonable as the slab begins to function more as a neutron reflector and thus the infinite medium albedo value is approached. The deuterium transmitted and reflected neutron leakage current spectra for the various slab thicknesses are depicted in Figs. 6 and 7. Table 3

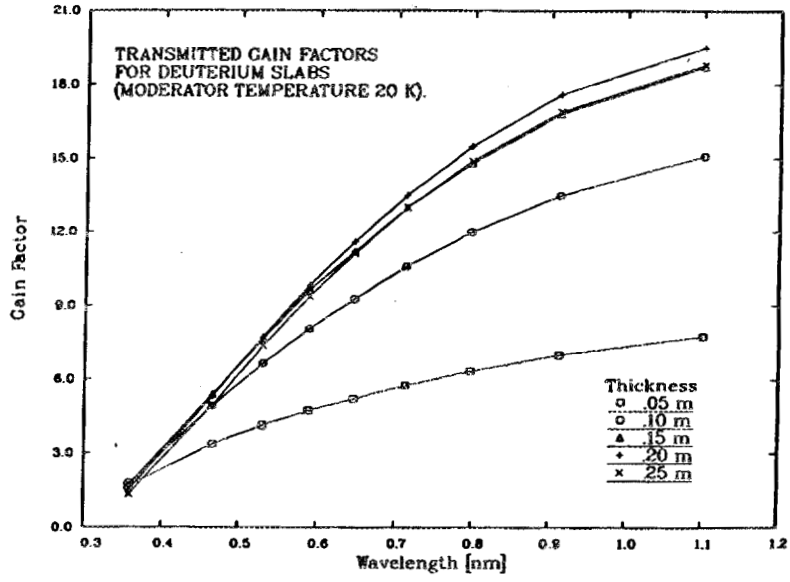

Figure 4. Transmitted gain factors for liquid deuterium slab moderators of thickness .05, .10, .15, .20, and .25 m.

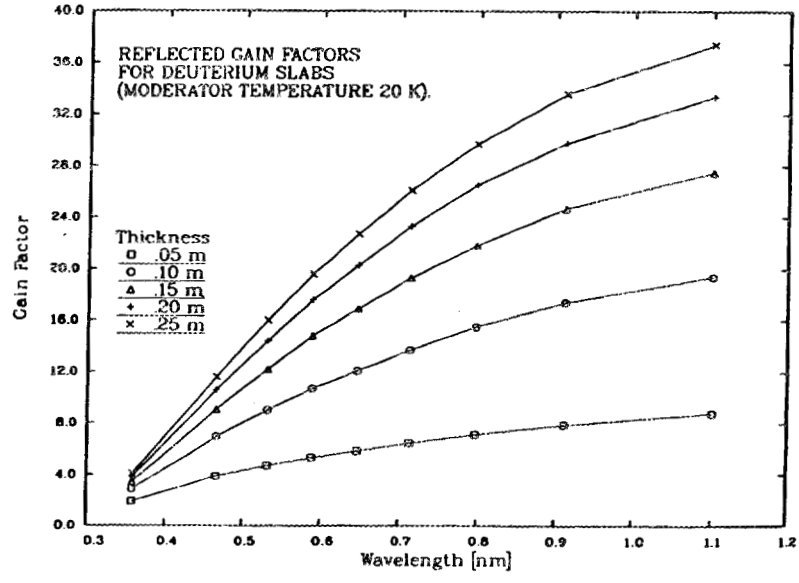

Figure 5. Reflected gain factors for liquid deuterium slab moderators of thickness .05, .10, .15, .20, and .25 m.

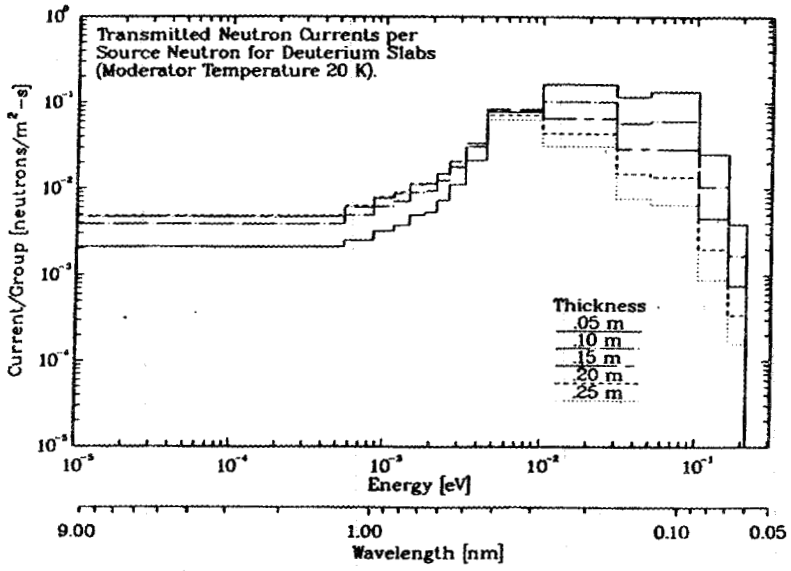

Figure 6. Transmitted neutron leakage current spectra for liquid deuterium slab moderators of thickness .05, .10, .15, .20, and .25 m.

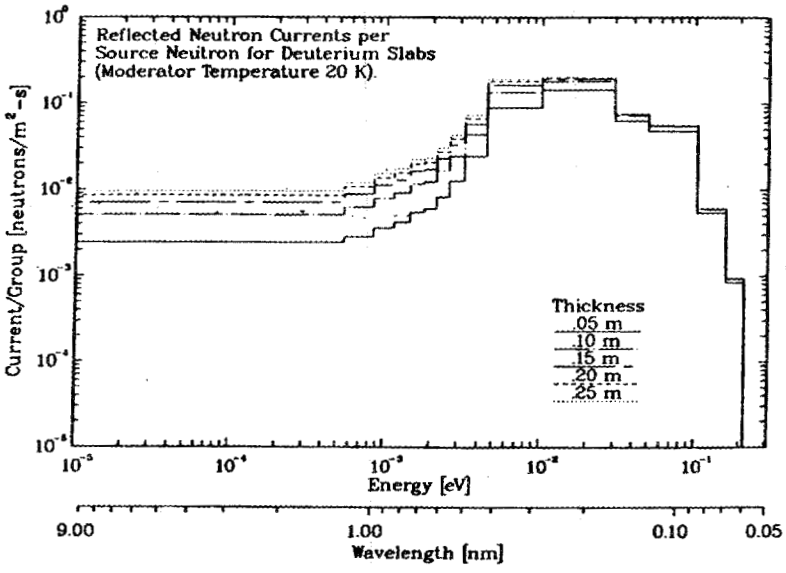

Figure 7. Reflected neutron leakage current spectra for liquid deuterium slab moderators of thickness .05, .10, .15, .20, and .25 m.

presents the transmitted and reflected cold neutron leakage currents below 10 meV for the various slab thicknesses.

Figures 8 and 9 depict the transmitted and reflected liquid nitrogen–15 cold neutron gain factor results. Above .80 nm, a slab having a thickness of .32 m achieves the maximum gain factor value though the difference from the .28 m slab value is small. Between .55 and .70 nm, slabs with thicknesses of .20, .24, .28, and .32 m give quite similar results. The liquid nitrogen–15 reflected gain factor results exhibit the same behavior as the liquid deuterium results; that is, the gain factor values increase at all wavelengths as the slab thickness increases. Figures 10 and 11 depict the transmitted and reflected neutron leakage current spectra for the various slab thicknesses. Table 4 presents the transmitted and reflected cold neutron leakage currents below 10 meV.

Comparing the liquid deuterium and the liquid nitrogen–15 results, one notes that the nitrogen–15 group gain factor results are considerably below the deuterium values. This difference in the gain factors is attributed to the difference in the temperature of the moderating materials (a colder moderator enhances the neutron fraction at longer wavelengths) and the difference in their atomic masses (neutron energy loss by elastic collisions is greater for lighter elements). Also, quite noticeable is that the reflected gain factors are larger than the transmitted values which is reasonable considering that neutron energy loss is greater for a neutron scattered in the backward direction. Furthermore, as a slab thickness increases, the slabs function more as a neutron reflector thus enhancing the reflected neutron component.

The question arises, how well do the transmitted and reflected leakage intensity spectra approach the energy spectrum of an ideal maxwellian at the moderator temperature? Figures 12 and 13 present a comparison of a maxwellian to the transmitted and reflected liquid deuterium (slab of thickness .20 m) leakage intensities and liquid nitrogen–15 (slab thickness of .28 m) leakage intensities, respectively. In both figures, the ideal maxwellian curve has been normalized to the transmitted intensity. For energies below 10 meV, the transmitted spectrum curves are below the ideal Maxwellian curve. If the maxwellian spectrum would have been normalized to the reflected intensity level, the reflected spectra curves would, for energies below 10 meV, also be below the ideal maxwellian curve. At the high energy end, the deviation from the ideal maxwellian is quite large. The deviations from the ideal maxwellian indicate the assymetry of the neutron source in relation to the moderator and are due, in part, to the finite size of the moderator.

From the one-dimensional slab geometry analysis given above, the optimum thickness for neutron transmission through a slab given an isotropic incident flux having a maxwellian room temperature energy distribution is, for wavelengths above .60 nm, approximately .20 m for liquid deuterium and between .28 and .32 m for liquid nitrogen–15.

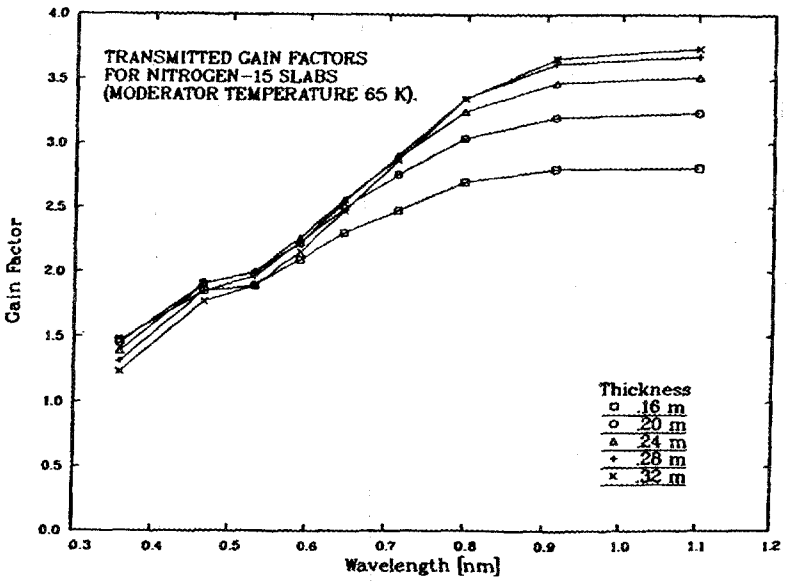

Figure 8. Transmitted gain factors for liquid nitrogen–15 slab moderators of thickness .16, .20, .24, .28, and .32 m.

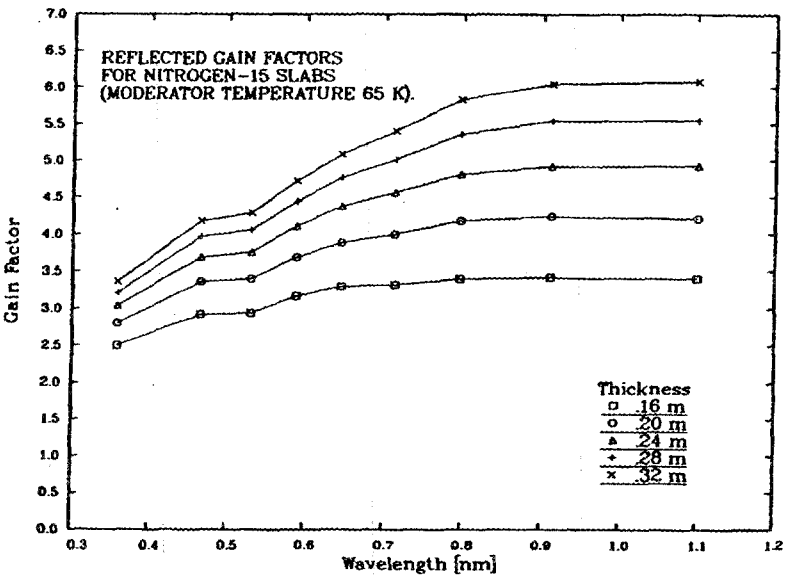

Figure 9. Reflected gain factors for liquid nitrogen–15 slab moderators of thickness .16, .20, .24, .28, and .32 m.

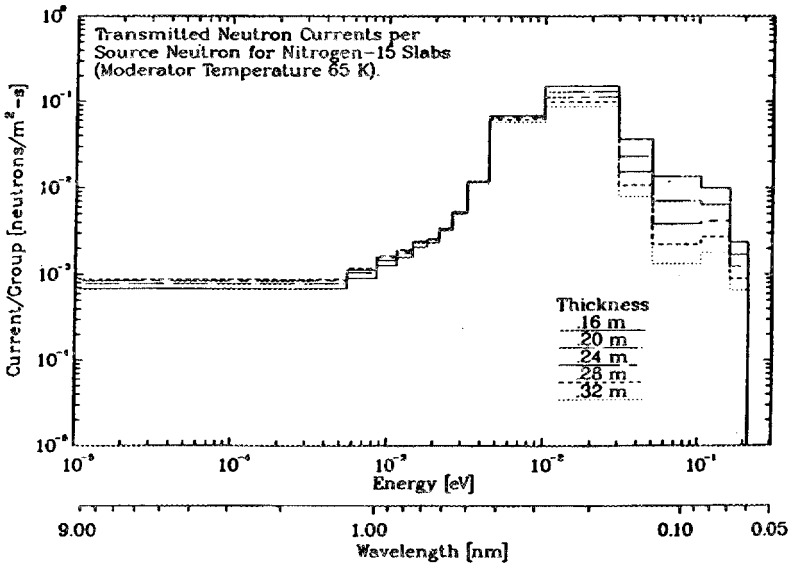

Figure 10. Transmitted neutron leakage current spectra for liquid nitrogen-15 slab moderators of thickness .16, .20, .24, .28, and .32 m.

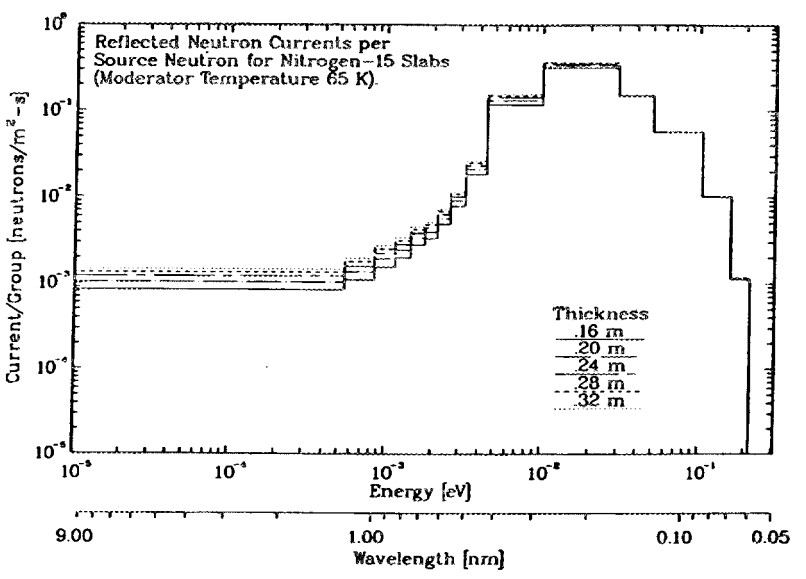

Figure 11. Reflected neutron leakage current spectra for liquid nitrogen-15 slab moderators of thickness .16, .20, .24, .28, and .32 m.

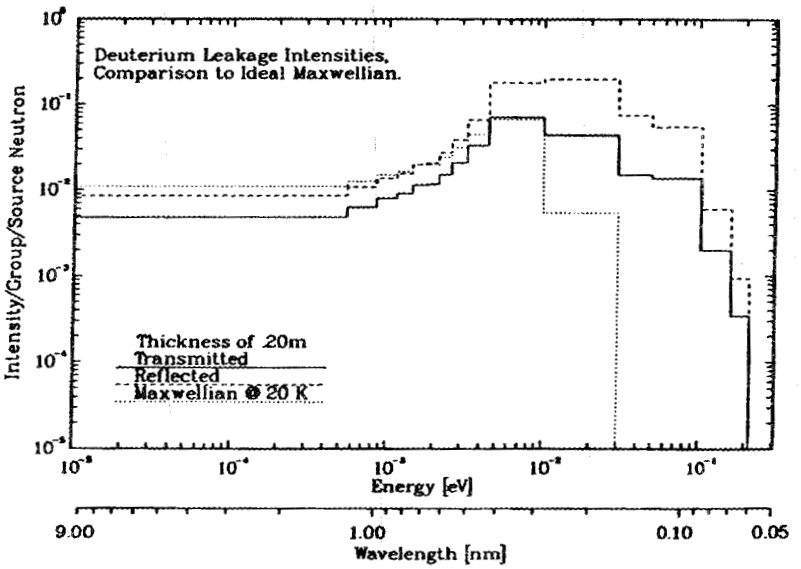

Figure 12. A comparison of the transmitted and reflected energy leakage intensities of a .20 m thick liquid deuterium slab to an ideal maxwellian energy distribution @ 20 K (normalized to the transmitted intensity).

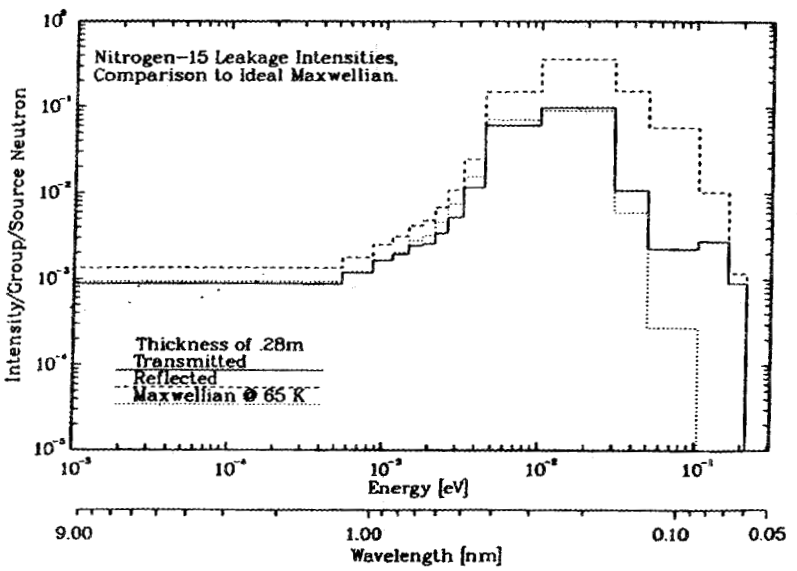

Figure 13. A comparison of the transmitted and reflected energy leakage intensities of a .28 m thick liquid nitrogen-15 slab to an ideal maxwellian energy distribution @ 65 K (normalized to the transmitted intensity).

Table 3

Cold Neutron Leakage Current/Source Neutron
Below 10 meV from Deuterium Slabs

Slab Thickness [m]	Transmitted Current [n/m^2-s]	Reflected Current [n/m^2-s]
.05	1.38×10^{-1}	1.58×10^{-1}
.10	1.84×10^{-1}	2.70×10^{-1}
.15	1.97×10^{-1}	3.46×10^{-1}
.20	1.91×10^{-1}	3.98×10^{-1}
.25	1.77×10^{-1}	4.34×10^{-1}

Table 4

Cold Neutron Leakage Current/Source Neutron
Below 10 meV from Nitrogen-15 Slabs

Slab Thickness [m]	Transmitted Current [n/m^2-s]	Reflected Current [n/m^2-s]
.16	9.71×10^{-2}	1.59×10^{-1}
.20	9.80×10^{-2}	1.81×10^{-1}
.24	9.58×10^{-2}	1.97×10^{-1}
.28	9.20×10^{-2}	2.10×10^{-1}
.32	8.73×10^{-2}	2.21×10^{-1}

3.2. SOLID SPHERE MODERATORS

The ideal situation of a moderator immersed within an isotropic and spatially uniform density flux of thermalized neutrons at room temperature is examined by a one-dimensional spherical geometry calculational model. For the parametric computations, solid spheres having diameters of .30, .34, .38, .42, .46, and .50 m are examined. A diameter of .38 m is currently being considered for the ANS cold source.

Figures 14 and 15 display the cold neutron gain factor results plotted according to their group midpoint wavelengths for liquid deuterium and liquid nitrogen–15 spherical moderators. For both moderators, the gain factors increase with sphere size. The increase is less for the same increase in step size indicating that there may be an optimum diameter which maximizes the gain factor for a given wavelength. As in the slab geometry computations, the liquid nitrogen–15 values are lower than the liquid deuterium values. The neutron leakage current spectra for the various diameter deuterium and nitrogen–15 spherical moderators are given in Figures 16 and 17. Table 5 presents the cold neutron leakage currents below 10 meV. One notes that the current decreases with increasing sphere size. This indicates that there is an optimum thickness which maximizes the neutron leakage current for a given wavelength.

The computed spherical geometry results are approximately a factor of 1.6 to 2.2 (at 1.1 nm) larger than the slab geometry transmission results. This is to be expected as in spherical geometry the transmitted and reflected leakages combine to determine the overall leakage intensity.

Table 5

Cold Neutron Leakage Current/Source Neutron
Below 10 meV from Deuterium and Nitrogen-15 Solid Spheres

	Leakage Current	
Diameter [m]	Deuterium [n/m^2-s]	Nitrogen-15 [n/m^2-s]
.30	1.58	7.05×10^{-1}
.34	1.30	5.83×10^{-1}
.38	1.08	4.91×10^{-1}
.42	9.17×10^{-1}	4.19×10^{-1}
.46	7.85×10^{-1}	3.62×10^{-1}
.50	6.79×10^{-1}	3.15×10^{-1}

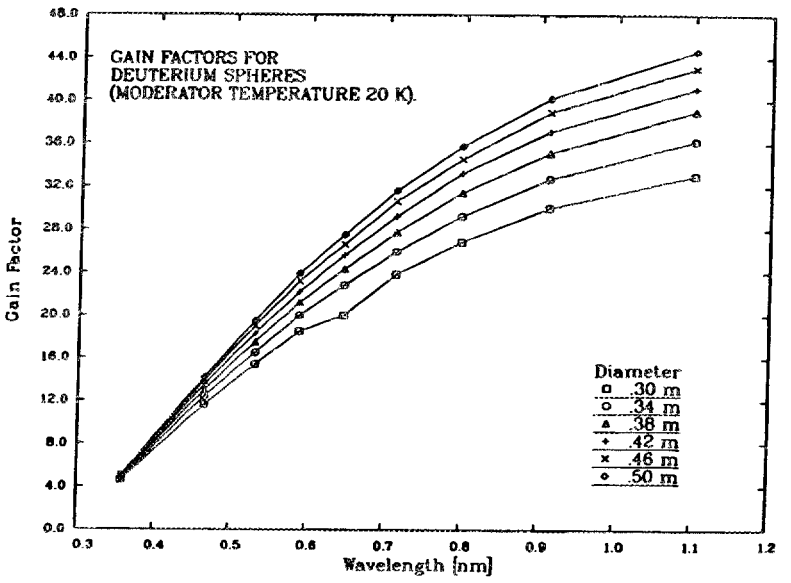

Figure 14. Gain factors for liquid deuterium spheres having diameters of .30, .34, .38, .42, .46, and .50 m.

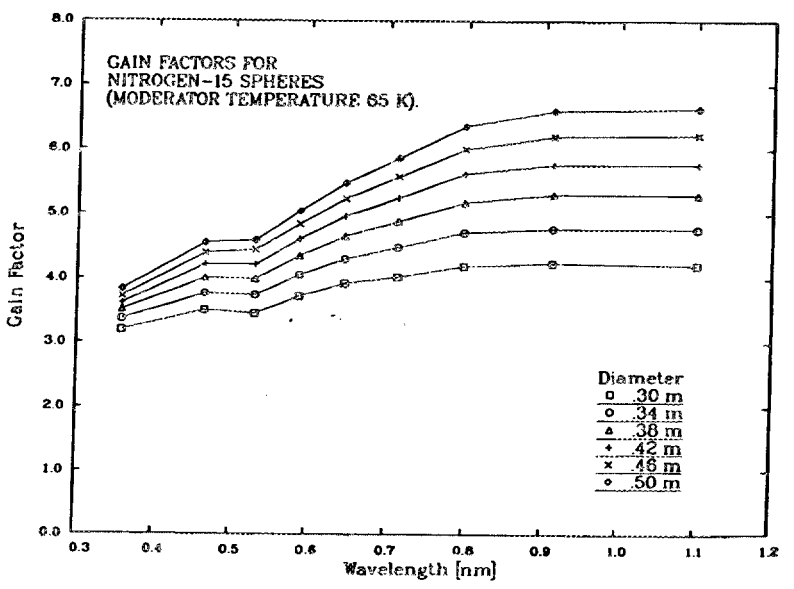

Figure 15. Gain factors for liquid nitrogen-15 spheres having diameters of .30, .34, .38, .42, .46, and .50 m.

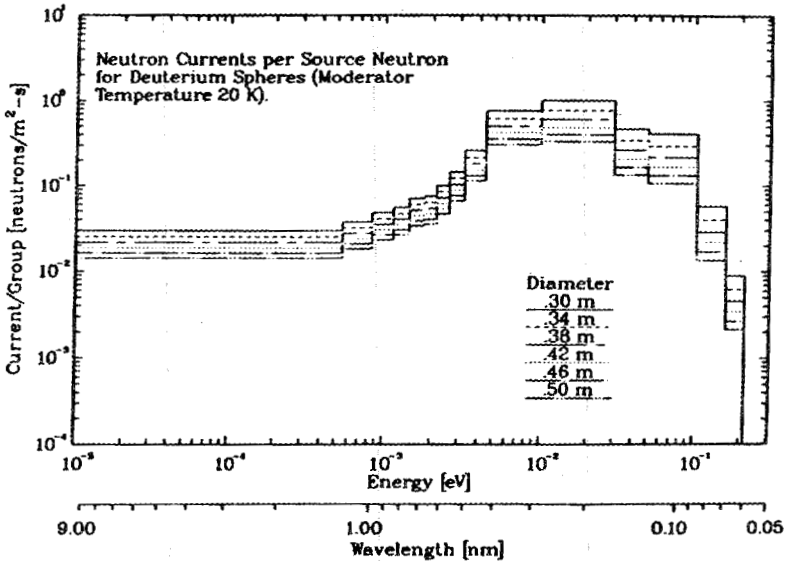

Figure 16. Neutron leakage current spectra for liquid deuterium spheres having diameters of .30, .34, .38, .42, .46, and .50 m.

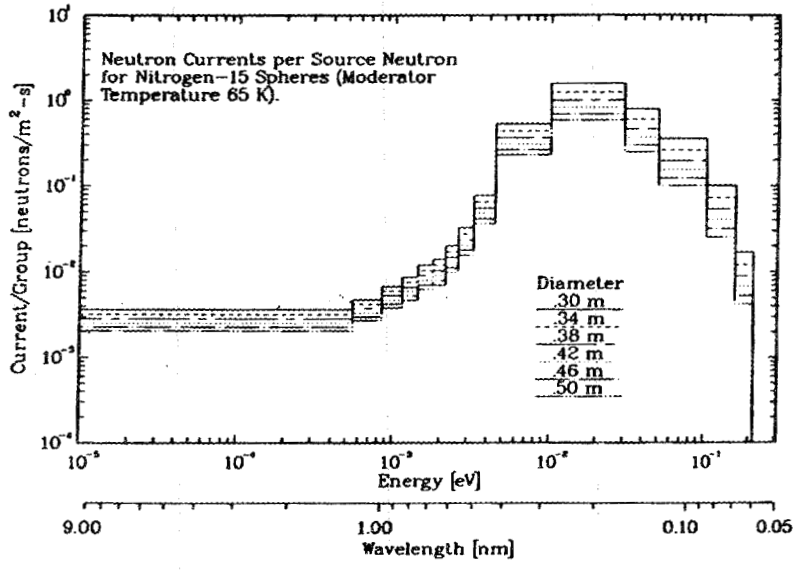

Figure 17. Neutron energy leakage current spectra for liquid nitrogen-15 spheres having diameters of .30, .34, .38, .42, .46, and .50 m.

3.3. SPHERICAL SHELL MODERATORS

In the previous subsection, cold neutron gain factor and leakage spectra results are reported for liquid deuterium and liquid nitrogen–15 solid sphere moderators. In this subsection, spherical shell moderators having an outer diameter equal to the currently considered cold source diameter of .38 m are investigated to determine their performance relative to the .38 m solid sphere case. Keeping the outer diameter fixed, spherical shells having inner radii of .04, .08, .12, and .16 m are considered. As in the solid sphere calculations, the spherical shell moderators are immersed within an isotropic and spatial uniform density flux of thermalized neutrons at room temperature. Of particular interest are the gain factor and neutron current spectra results of the neutrons entering the void region as one hopes to gain an understanding of the unusual shape of the cold source installed at the Institut Laue-Langevin (ILL) in France [15].

To investigate the effect that a central void region within the spherical moderators has on the gain factor and the neutron leakage current spectra results (neutron current into the void region and from the sphere), two spherical shell calculational models containing a central void region and a central black region are considered. From the central void region case, we obtain the overall gain factor and neutron current spectra results for the spherical shell; that is, the combined result of both the neutron component that has transversed the void region (either enter the void region directly as uncollided neutrons or are scattered into the void region) and the component that has not transversed the void region. In one-dimensional spherical calculations, this is simulated by a reflective boundary condition at the inner surface of the shell. The central black region case allows us to obtain information on the neutron component that is entering the void region. This is simulated by a vacuum boundary condition at the inner surface of the shell.

Figure 18 displays the liquid deuterium cold neutron gain factor results for the spherical shells containing a central void region. As can be discerned, the overall gain factor increases with increasing shell thickness. The .12 m shell values are slightly lower than the .16 m values. If one were to go with the .08 m shell, then one would reduce the liquid deuterium inventory by approximately 19% from the solid sphere case with the gain factor value reduced from approximately 35 to 31.5 at .9 nm. The liquid nitrogen-15 neutron gain factor results are displayed in Fig. 19. The liquid nitrogen-15 results are similar to the liquid deuterium results except for the lower gain factor values. Table 6 presents both the liquid deuterium and liquid nitrogen-15 cold neutron leakage currents below 10 meV for the various shell thicknesses.

Figure 20 displays the liquid deuterium gain factor results for the neutron component that is entering the void region computed from the spherical shell calculational model containing a central black region. In the figure, one notes that both the .08 and .12 m curves cross over the .04 m curve. This is a spectrum effect and is due to both the amount of neutron moderation taking place prior to entering

the void region and to the surface area of the void region (the surface area seen by the neutrons decreases with increasing shell thickness). The gain factors increase at longer wavelengths for an increase in the shell thickness from .04 to .08 m and decrease as one goes to .12 and then .16 m. This indicates that there is an optimum shell thickness for the gain factors at a given wavelength for neutron transmission into the void region and is consistent with early slab geometry calculations where an optimum thickness for neutron transmission was found. Due to curvature, the optimum thickness in spherical geometry will not necessarily be the same as for the slab geometry case. The neutron current spectra for the neutron component leaking into the void region is given in Fig. 21.

Figure 22 displays the liquid nitrogen–15 gain factor results for the neutron component that is entering the void region. As opposed to the deuterium inner surface results, the nitrogen–15 curves do not cross over; instead, the gain factors decrease with increasing shell thickness. The reason for not having a cross over is still being investigated, but it is believed that it may be related to the amount of energy lost on average per collision (a neutron scattered [elastically] from nitrogen–15 does not lose as much energy on the average as a neutron scattered from deuterium. This is due to the difference in their atomic masses). The neutron current spectra for the neutron component leaking into the void region is given in Fig. 23.

Table 7 presents the liquid deuterium and liquid nitrogen-15 cold neutron current spectra below 10 meV for the neutron component that is entering the void region. From the values given, one notes that the neutron current increases as the void region decreases. The neutron current below 10 meV for a .16 m thick spherical shell is slightly larger than that of the .38 m diameter solid sphere (see Table 5). According to Figures 14, 15, 20, and 21, however, the gain factor values for the .38 m solid sphere are substantially larger than the .16 m thick spherical shell values. Thus, for the maxwellian energy and spatially uniformly distributed isotropic flux used in the one-dimensional calculations, the solid sphere configuration is preferred. However, for the actual ANS reactor and cold source configuration, this may not be the case as the spatial distribution of the thermal neutron flux (source for the production of cold neutrons) has gradients in both the radial and axial directions (which cannot be modeled in one-dimensional calculations). In addition, the flux spectrum is non-maxwellian, i.e., shifted to higher neutron energies. These differences may lead to a different preference for the actual ANS cold source geometry.

At this point we would like to speculate on the reasoning for a cavity region and its effect on the neutron leakage and streaming down the beam guide. Figure 24a shows a schematic of the cold source moderator (R_0 = .19 m) and a beam guide (not drawn to scale). From Fig. 24a, one observes that the number of neutrons entering the beam guide is both a function of the spherical surface area seen by the beam guides and the neutron angular distribution on the spherical surface. Hence, it is possible that an introduction of a cavity region within the

Table 6

Cold Neutron Leakage Current/Source Neutron
Below 10 meV from Spheres (Diameter .38 m)
Containing a Central Void Region

Shell Thickness [m]	Leakage Current Deuterium [n/m^2-s]	Leakage Current Nitrogen-15 [n/m^2-s]
.04	7.80×10^{-1}	3.44×10^{-1}
.08	1.02	4.51×10^{-1}
.12	1.07	4.84×10^{-1}
.16	1.08	4.91×10^{-1}

Table 7

Cold Neutron Leakage Current/Source Neutron
Below 10 meV for Neutron Component Entering
Void Region (Outer Sphere Diameter .38 m)

Shell Thickness [m]	Leakage Current Deuterium [n/m^2-s]	Leakage Current Nitrogen-15 [n/m^2-s]
.04	3.27×10^{-1}	1.70×10^{-1}
.08	5.92×10^{-1}	2.62×10^{-1}
.12	9.16×10^{-1}	3.85×10^{-1}
.16	1.36	5.51×10^{-1}

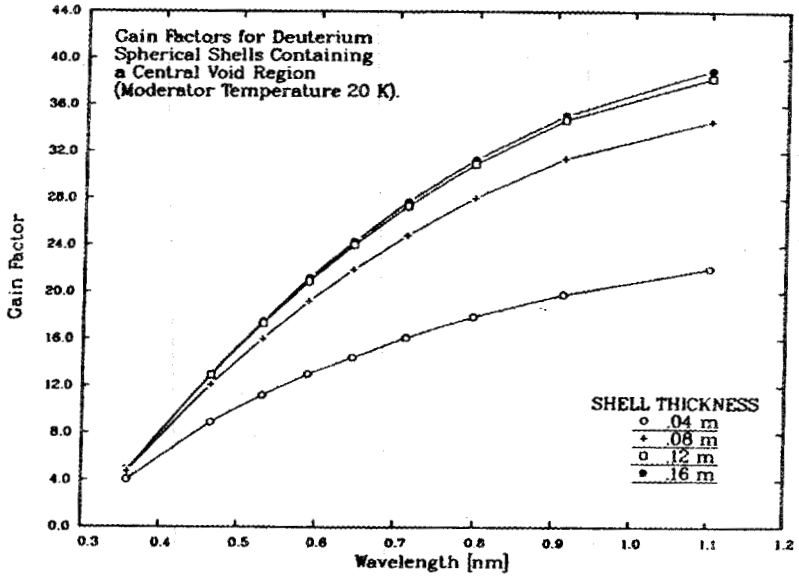

Figure 18. Gain factor results for liquid deuterium spherical shells containing a central void region for shells of thickness .04, .08, .12, and .16 m.

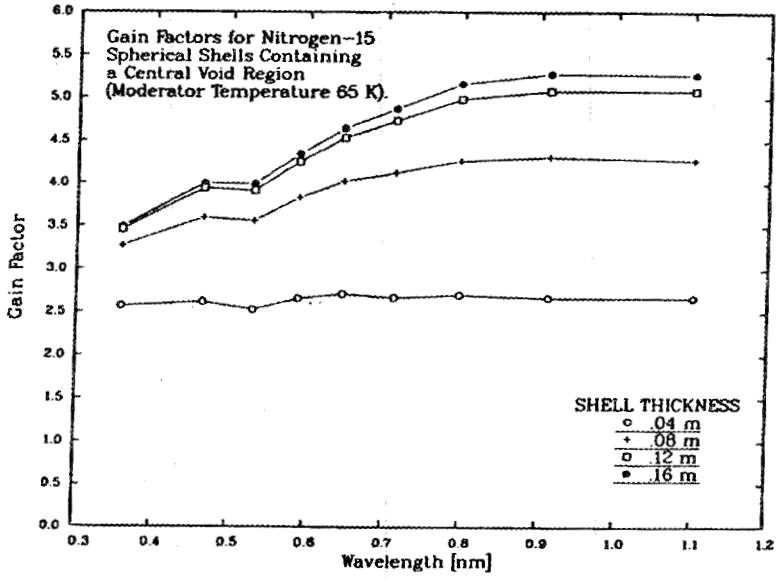

Figure 19. Gain factor results for liquid nitrogen-15 spherical shells containing a central void region for shells of thickness .04, .08, .12, and .16 m.

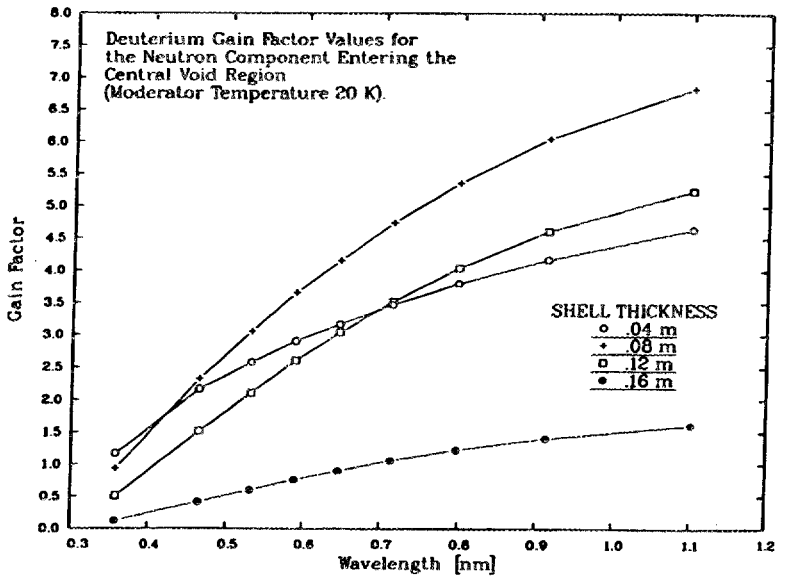

Figure 20. Liquid deuterium gain factor results for the neutron component entering the void region for shells of thickness .04, .08, .12, and .16 m.

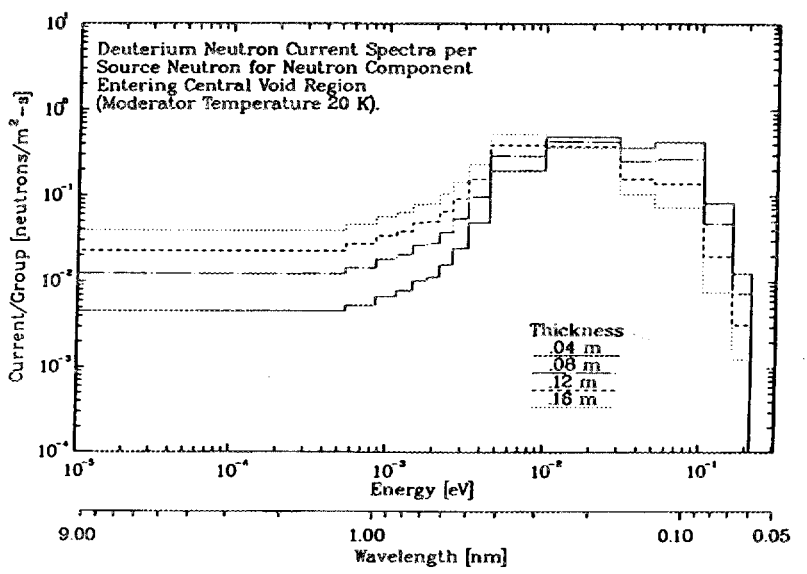

Figure 21. Liquid deuterium neutron current spectra for the neutron component entering the void region for shells of thickness .04, .08, .12, and .16 m.

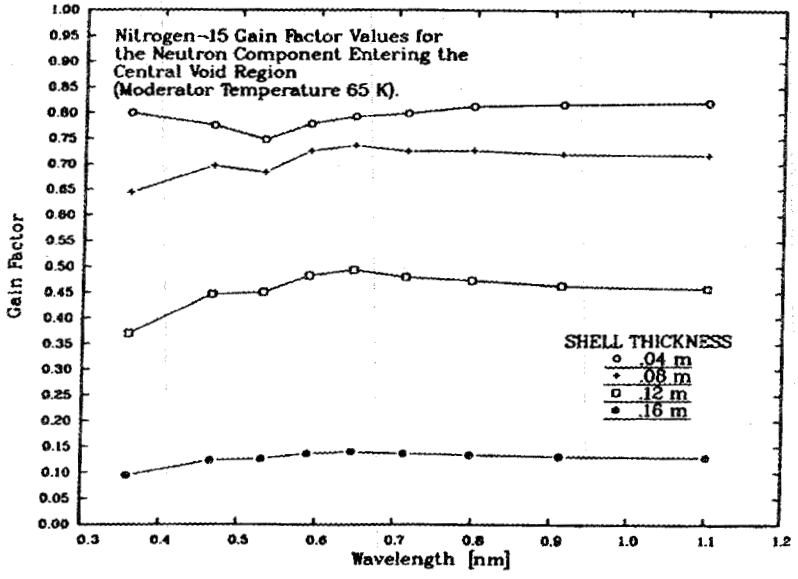

Figure 22. Liquid nitrogen-15 gain factor results for the neutron component entering the void region for shells of thickness .04, .08, .12, and .16 m.

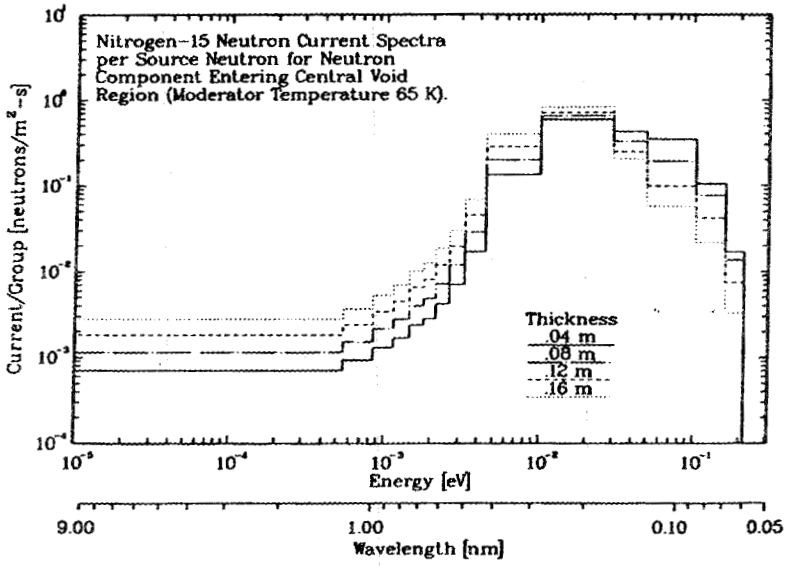

Figure 23. Liquid nitrogen-15 neutron current spectra for the neutron component entering the void region for shells of thickness .04, .08, .12, and .16 m.

cold neutron source accompanied by a change in the angular distribution of the emitted neutrons preferentially in the forward direction (directed down the beam guide) and additionally having the neutrons emitted in the selected energy range, could increase the neutron intensity at the end of the beam guide. Evidently, this has found success in the new French ILL Cold Source moderator where they have reported a factor of 2.1 [15] increase in the cold flux intensity by inclusion of a cylindrically shaped cavity (see Fig. 24c). Additionally, according to the above simple spherical geometry analysis, it is possible to increase the cold neutron current by introduction of a cavity.

Figures 24b through 24e depict various shapes of possible cavities. The formulae for the surface area of the cavities is given next to the shapes. The shape of the cavity is of importance as it effects the angular distribution of the emitted neutrons. To examine this effect one must resort to multidimensional transport calculations where additionally it is possible to model the flux spatial gradients in the radial and axial directions.

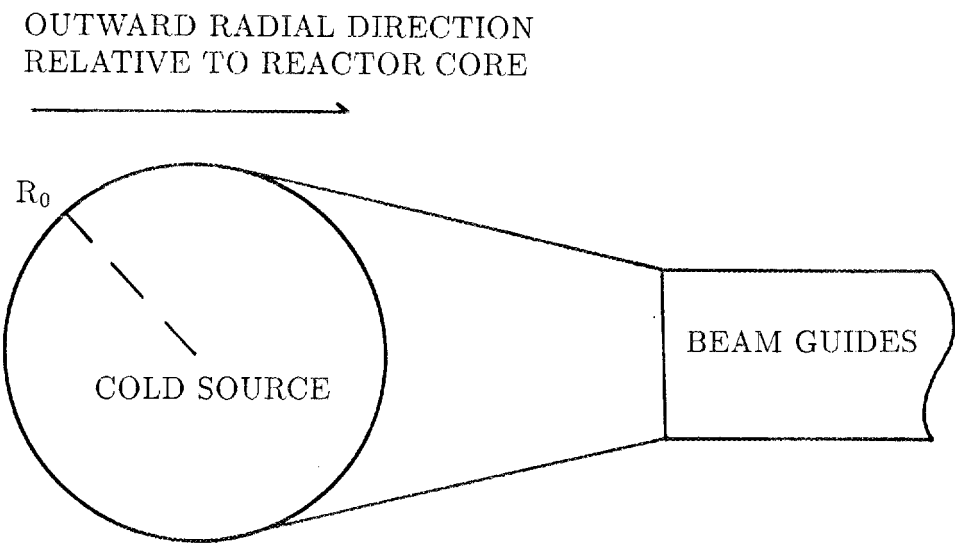

Figure 24a. Cold source moderator and beam guide arrangement.

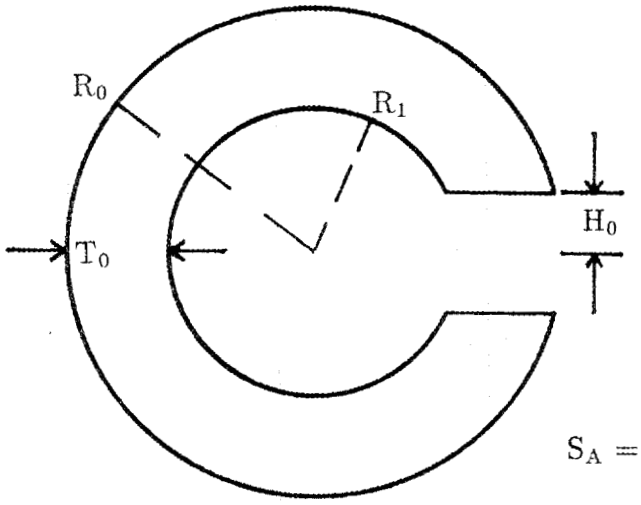

$$S_A = 2\pi R_1(R_1 + \sqrt{(R_1^2 - H_0^2)} + 2\pi H_0 T_0$$

Figure 24b. Case 1: Concentric spherical cavity.

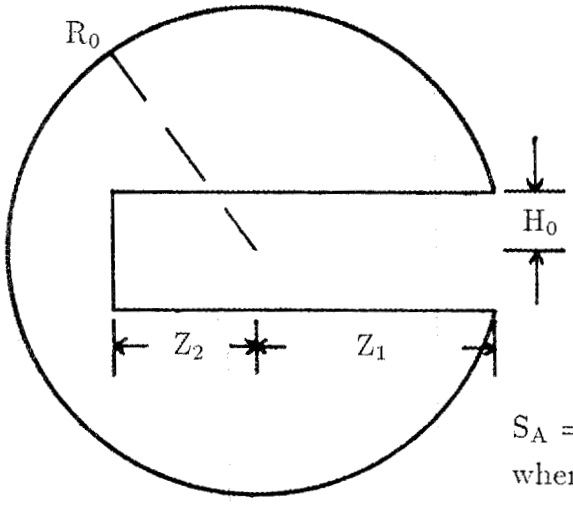

$$S_A = 2\pi H_0(Z_1 + Z_2) + H_0^2\pi$$
where $Z_1 = \sqrt{R_0^2 - H_0^2}$

Figure 24c. Case 2: Cylindrical cavity.

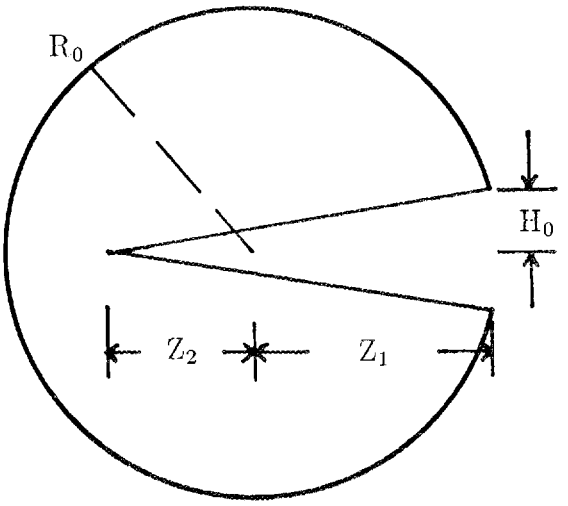

$$S_A = \pi H_0 \sqrt{Z_0^2 + H_0^2}$$
where $Z_0 = Z_1 + Z_2$
and $Z_1 = \sqrt{R_0^2 - H_0^2}$

Figure 24d. Case 3: Conical cavity.

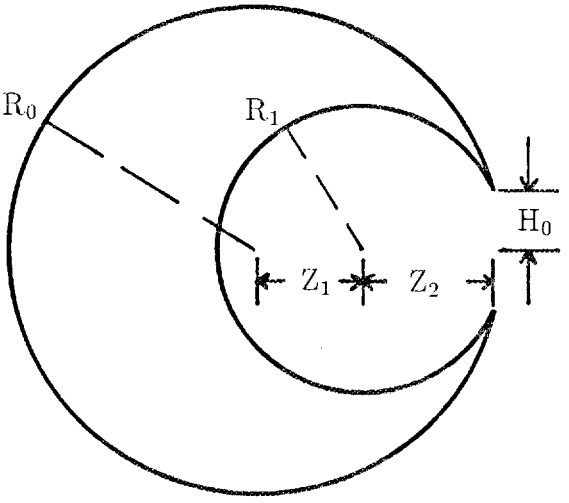

$$S_A = 2\pi R_1(R_1 + Z_2)$$
where $Z_2 = \sqrt{R_1^2 - H_0^2}$
and $Z_1 + Z_2 = \sqrt{R_0^2 - H_0^2}$

Figure 24e. Case 4: Offset spherical cavity.

4. SUMMARY

Simple one-dimensional slab and spherical geometry parametric calculations have been performed to investigate the performance of a possible liquid nitrogen–15 versus a liquid deuterium cold source moderator. The gain factors computed for the liquid nitrogen–15 cold source (@ 65 K) are considerably below those computed for the much colder liquid deuterium cold source (@ 20 K), as is reasonable considering the difference in moderator temperatures and atomic masses. Nevertheless, nitrogen–15 does represent a viable option should safety-related issues prohibit the use of deuterium as a moderating material. Liquid nitrogen-15 is also a viable candidate for a cool neutron source.

The slab geometry calculations have indicated that the optimum thickness for neutron transmission through a slab given an isotropic incident flux having a maxwellian room temperature energy distribution is, for wavelengths above .60 nm, approximately .20 m for liquid deuterium and between .28 and .32 m for liquid nitrogen–15. Also, the reflection of neutrons was seen to be the dominant moderating mechanism, and hence a cold source design enhancing the reflection of neutrons should be considered.

The ideal situation, that of a moderator immersed within an isotropic and spatially uniform density flux of neutrons was investigated by the solid sphere and spherical shell calculational models. For the spherical sizes considered in the analysis, the gain factors at a given wavelength increased with sphere size but the cold neutron current below 10 meV decreased with increasing sphere size. This indicates that there is an optimum diameter which maximizes the neutron leakage current for a given wavelength.

The spherical shell calculations have indicated that the cold neutron current below 10 meV for the neutron component entering a cavity region can exceed the neutron leakage current (below 10 meV) from the exterior of a solid sphere. In particular, the neutron current into the cavity region of a .16 m thick spherical shell (outer diameter .38 m) exceeds the neutron leakage current from the .38 m diameter sphere currently being considered for the ANS reactor cold source. However, the cold neutron gain factors are considerably lower than for the solid sphere case. To assess properly the question, cavity or no cavity, multi-dimensional transport calculations with more realistic spatial and energy source distributions as encountered in the ANS reactor are required.

5. ACKNOWLEDGMENTS

The author has benefitted from discussions with T. A. Gabriel, Y. Y. Azmy, and R. A. Lillie of the Engineering Physics and Mathematics Division. Thanks to F. J. Peretz for the preparation and use of Figure 1.

REFERENCES

1. D. L. Selby et al., "ORNL Contributions to the Advanced Neutron Source (ANS) Project for October 1986–March 1987," ORNL/TM-10579, Oak Ridge National Laboratory, Oak Ridge, Tennessee (November 1987).
2. Dr. John Hayter, "Liquid Nitrogen-15 Cold Neutron Moderator," DOE Invention Disclosure E/SID 417-X (December 1987).
3. J. A. Young and J. U. Koppel, "Slow Neutron Scattering by Molecular Hydrogen and Deuterium," *Phys. Rev.,* **135**, p. A603 (August 1964).
4. J. W. Arwood et al., "Preparation and Benchmarking of ANSL-V Cross Sections for Advanced Neutron Source Reactor Studies," *Trans. Am. Nucl. Soc.,* **55** p. 615 (November 1987).
5. W. D. Seiffert, "Measurement of Scattering Cross Sections of Liquid and solid Hydrogen, Deuterium and Deuterium Hydride for Thermal Neutrons," EUR-4455d (1970).
6. M. Utsuro, "Slow Neutron Scattering and Intermolecular Excitations in Liquid Hydrogen," *Z. Physik B* **27**, p. 111 (1977).
7. M. Utsuro and M. Hetzelt, "Liquid Ortho-Deuterium as a Converter for Ultra-Cold Neutrons," In *Neutron Inelastic Scattering*, Vol. 1, Wien, IAEA-SM-219/63, p. 67 (1977).
8. W. Bernnat, D. Emendörfer, J. Keinert, M. Mattes, "Evaluation of Neutron Cross Sections for Liquid Hydrogen and Deuterium for the Design of Cold Neutron Sources," Proceedings of the International Conference on Nuclear Data for Science and Technology, Mito, Japan, May 30-June 3, 1988.
9. Dr. John Hayter, private communication.
10. V. F. Sears, "Theory of Cold Neutron Scattering by Homonuclear Diatomic Liquids, I. Free Rotations," *Canadian J. of Phys.,* **44** p. 1279 (1966).
11. V. F. Sears, "Theory of Cold Neutron Scattering by Homonuclear Diatomic Liquids, II. Hindered Rotations," *Canadian J. of Phys.,* **44** p. 1299 (1966).
12. A. H. Narten et al., "Atom Pair Potentials of Liquid Nitrogen from Diffraction Data," *J. of Chem. Phys.,* **73** p. 1248 (August 1980).
13. W. W. Engle, Jr., "A Users Manual for ANISN, A One-Dimensional Discrete Ordinates Transport Code with Anisotropic Scattering," K-1693, Union Carbide Corporation, Nuclear Division, (March 1967).

14. W. A. Rhoades and R. L. Childs, "DOT-4.3, An Updated Version of the DOT 4 One- and Two-Dimensional Neutron/Proton Transport Code," ORNL-5851, Oak Ridge National Laboratory (April 1982).

15. T. Springer, "The Installation of a Second Cold Source in the High Flux Reactor at the Institut Laue-Langevin," Institut Max Von Laue Paul Langevin, 81SP49S, Grenoble (September 1981).

INTERNAL DISTRIBUTION

1. R. G. Alsmiller, Jr.
2. Y. Y. Azmy
3. F. C. Difilippo
4. F. F. Dyer
5. W. R. Gambill
6. R. M. Harrington
7. J. B. Hayter
8–12. D. L. Henderson
13. J. A. Johnson
14. R. A. Lillie
15. F. C. Maienschein
16. B. H. Montgomery
17. F. R. Mynatt
18. F. J. Peretz
19. R. T. Primm, III
20. H. Reutler
21. T. L. Ryan
22. D. L. Selby
23. P. B. Thompson
24. K. R. Thoms
25. M. K. Wilkinson
26. C. D. West
27. G. T. Yahr
28. G. L. Yoder
29. EPMD Reports Office
30–31. Laboratory Records Department
32. Laboratory Records, ORNL-RC
33. Document Reference Section
34. Central Research Library
35. ORNL Patent Office

EXTERNAL DISTRIBUTION

36. Dr. John J. Dorning, Department of Nuclear Engineering and Engineering Physics, Thornton Hall, University of Virginia, Charlottesville, Virginia 22901
37. B. Chalmers Frazer, Materials Science Division, U.S. Department of Energy, Germantown, ER-132, Washington, D.C. 20545
38. Ralph Fullwood, Brookhaven National Laboratory, Upton, New York 11973
39. Dr. Robert M. Haralick, Department of Electrical Engineering, University of Washington, Seattle, Washington 98195
40. J. A. Lake, Manager, Nuclear Engineering and Reactor Design, Idaho National Engineering Laboratory, P.O. Box 1625, Idaho Falls, Idaho 83415
41. John M. Ryskamp, Idaho National Engineering Laboratory, P.O. Box 1625, Idaho Falls, Idaho 83415
42. J. L. Snelgrove, Argonne National Laboratory, 9700 South Cass Avenue, Argonne, Illinois 60439
43. Iran Thomas, Director, Materials Sciences Division, U.S. Department of Energy, Germantown, ER-13, Washington, D.C. 20545
44. D. K. Wilfert, Energy Programs, U.S. Department of Energy, Oak Ridge Operations, P.O. Box E, Oak Ridge, Tennessee 37831

45. R. J. Willard, U.S. Department of Energy, Oak Ridge Operations, P.O. Box E, Oak Ridge, Tennessee 37831
46. Office of Assistant Manager, for Energy Research & Development,, DOE-ORO,, Oak Ridge, TN 37830

47–56. Office of Scientific and Technical Information, P.O. Box 62, Oak Ridge, Tennessee 37830